Jordan Journal of Civil Engineering, Volume **20**, No. **3**, **2026**
DOI: https://doi.org/10.14525/JJCE.v20i3.07

Jordan Journal of Civil Engineering

Journal homepage: https://jjce.just.edu.jo

Laboratory Investigation of Marine Sandy Soil with Reinforcement and Variation of Saturation under Shaking

Aicha Boukhalfa [1)*], ***Mohammed Bousmaha*** [1),2)], ***Abdelkader Hachichi*** [1),2)]

[1)] *Department of Civil Engineering, University of Science and Technology of Oran - Mohammed Boudiaf, 31000, Algeria.*
** Corresponding Author, E-Mail: aicha.boukhalfa@univ-usto.dz*
[2] *Materials, Soils and Thermal Laboratory, University of Science and Technology of Oran - Mohammed Boudiaf, 31000 (Algeria). E-Mails: mohammed.bousmaha@univ-usto.dz; abdelkader.hachichi@univ-usto.dz*

ARTICLE INFO

Article History:
Received: 29/8/2025
Accepted: 9/1/2026

ABSTRACT

This study investigates the mechanical improvement of sandy soils reinforced with synthetic fibers under vibrational loading. Experimental work was conducted on an undrained non-cohesive soil with two relative densities (loose and medium-dense) and varying saturation degrees. Fiber-reinforced and natural sands were first characterized in static triaxial tests, and the selected fiber contents were subsequently tested under dynamic excitation. Dynamic response was assessed by applying accelerations comparable to those recorded during the CHI-CHI earthquake (Taiwan, 1999). The results demonstrate that fiber adding enhances the strength and stiffness of sand, thereby mitigating its vulnerability to seismic loading. Additionally, the interaction between relative density and saturation degree was found to strongly influence the soil's overall mechanical behavior. This work confirms the efficiency of fiber reinforcement as a soil improvement technique for reducing seismic risks in sandy deposits.

Keywords: Sandy soils, Vibrational mode, Synthetic fibers, Relative density, Saturation degree.

INTRODUCTION

Sandy soils, which are generally classified as non-cohesive soils, are widely used in civil engineering projects. They are often utilized in foundations, embankments and dikes. It should be noted that the granular structure of sandy soils lacks natural cohesion, making them particularly sensitive to mechanical stresses, especially under undrained conditions. Furthermore, the lack of cohesion in sandy soils can lead to significant instabilities or deformations. This is particularly true during rapid loadings, such as those caused by vibration stresses resulting from earthquakes, which manifest as ground vibrations following the propagation of seismic waves. Moreover, the presence of water in soil can accentuate these instabilities which can engender a risk of liquefaction (Kousar et al., 2023; Nozomu, 2024), whether in the case of static or dynamic loading (Bouafia, 2010; Yu et al., 2017).

The study of parameters related to natural hazards can be done in the laboratory using the triaxial apparatus or a shaking table (Benghalia, 2018; Beena et al., 2019), and in situ by analyzing the correlations between the penetration tests (Cone Penetration Test – CPT and dynamic penetration test-DPT) and dynamic polling (DP). The findings can then be used for the static and dynamic characterization of soil to better understand its behavior under various loading conditions, thereby

improving its characteristics (Chang & Chou, 2019; Santos & Bicalho, 2022). In this context, Terzaghi was the first to explain the phenomenon of soil liquefaction through the study of geohazards. It is worth emphasizing that during an earthquake, contacts between solid soil particles are often disturbed in non-cohesive soils in the presence of interstitial water (Arab & Shahrour, 2009). In addition, consolidation of saturated sediments, under undrained conditions, does not occur and the pore pressure increases as soil density changes due to the rearrangement of soil grains. Finally, the effective stress supported by sediments decreases as pore pressure increases, allowing the solid weight to be entirely supported by the pore water; consequently, the sediments become fluid (Goren et al., 2013). It should also be noted that, in marine constructions, the risk of liquefaction can occur at the soil surface and spread rapidly until reaching an impermeable layer. In this case, the soil behaves like a liquid. This phenomenon often appears after earthquakes. This topic has been widely investigated over the last thirty years. In this context, a large number of research studies have been conducted on the impact of liquefaction resulting from the vibrational excitation of soil (Sumer et al., 2012). It is noteworthy that significant advances have been made in the field of marine structures (Jeng et al., 2013). The findings have significantly contributed to predicting the behavior of liquefiable soils. In addition, several factors affecting the behavior of liquefiable soils have been studied (El Shamy & Zeghal, 2007; Sawicki, 2009; Taiba, 2017; Leak & Barreto, 2024).

On the other hand, the precise determination of critical conditions, such as the initial void ratio, the degree of saturation, the content of fine and coarse elements in soil, has been a major challenge for geotechnical engineers. In addition, the characteristics of vibrations, such as the frequency and amplitude, are among the most important factors for controlling the mechanical instability and large mass displacements of soil (Seed et al., 2001; El Ouni et al., 2013; Ozbay & Cabalar, 2016; Sun et al., 2018). These factors can be used to predict the liquefaction or expansion behavior of porous soil in order to avoid instability risks, which manifest as failure or large-scale displacement. (Sun et al., 2017). Moreover; the risk of instability most often affects sands with medium or low density. For the purpose of overcoming these weaknesses, many soil improvement techniques have been developed. Among these techniques, fiber reinforcement, which has emerged as an innovative and relatively simple solution, deserves to be mentioned. It is noteworthy that the concept of soil reinforcement was first introduced by Henri Vidal as part of the reinforced soil technique that he invented and developed in the early 1960s (Schlosser et al., 1984). Since then, a large number of fiber reinforcement techniques of soil using geosynthetic fibers (Kakaa & Taki, 2008; Nouri et al., 2009; Nouri et al., 2015; Brahim, 2017; Shiva & Kumar, 2018; El zamel et al., 2023,), glass fibers (Bouaricha & Djafar, 2015; Bouaricha et al., 2018), natural fibers (Ghembaza et al., 2023), as well as hydraulic binders (Boutouba, 2021) have gained considerable research momentum. It has been reported that the addition of fibers in a sandy matrix allows creating some mechanical interaction between the sand grains and fibers, thus ensuring a pseudo-cohesion that helps improve the resistance of sand.

Consequently, to characterize soil and select the most appropriate fiber percentage, unconsolidated undrained (UU) triaxial tests were conducted to analyze the mechanical behavior of saturated sands in vibrational mode as a function of the variation of the saturation degree (Della et al., 2010), before and after fiber addition. These tests, which were carried out on a shaking table, made it possible to assess the short-term behavior of soil under undrained conditions, based on the vibration model of the 1999 Chi-Chi earthquake in Taiwan.

MATERIALS AND METHODS

Characterization of the Sand and Fibers Used

It is worth emphasizing that the sand used in this study is natural sand, sourced from the eastern region of the city of Oran (Coastal srtip). This is coarse, clean, and poorly graded sand that is classified as poorly-graded sand (SP), according to the USCS classification (ASTM D2487). Figure 1 shows its grain size distribution curve.

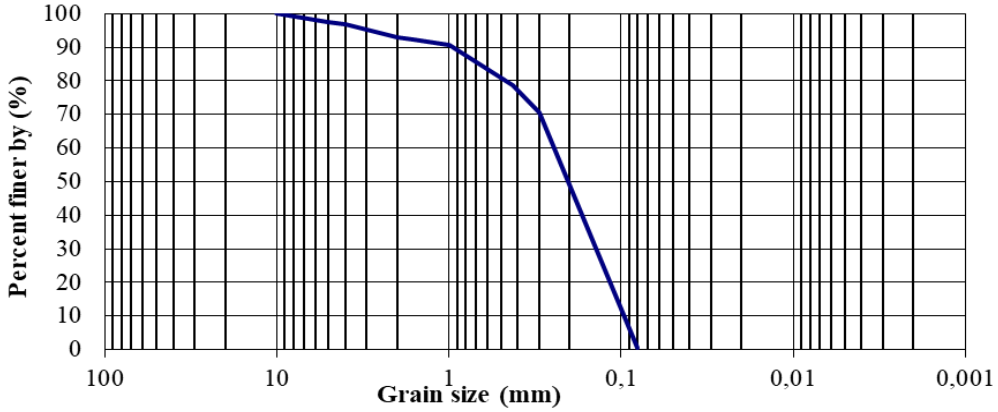

Figure 1. Grain size distribution curve of the studied soil

Figure 2 shows the grain size distribution of the studied soil which ranges within boundaries of the potentially liquefiable and the most liquefiable soils, as established by Tsuchida (1970).

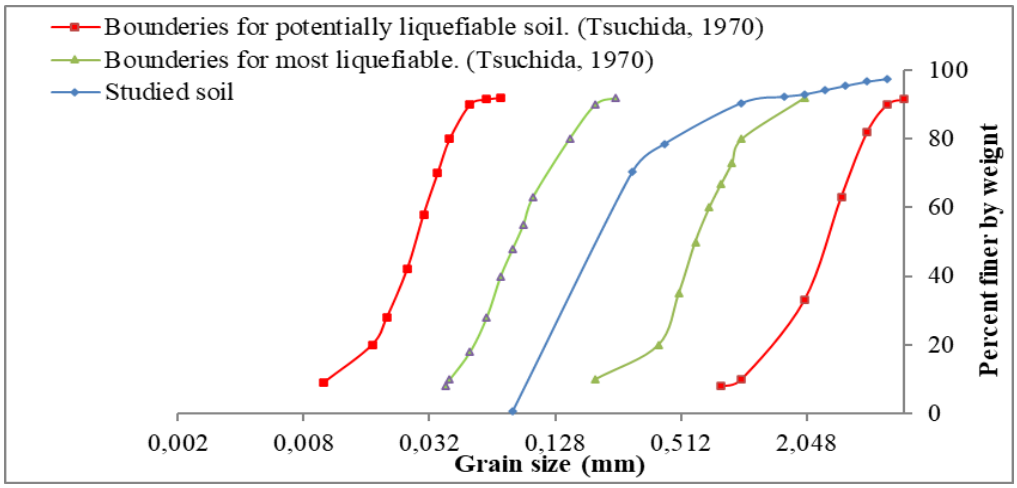

Figure 2. Particle size distribution of the studied soil and the boundaries of the liquefiable soils (Tsuchida, 1970)

Furthermore, the results of the physico-chemical tests and soil properties are all presented in Table1.

Table 1. Geotechnical properties of sand

Sampling description	Reference	Results
< to 0.075 mm	ASTMD-422	0.60
D_{60} (mm)	ASTMD-422	0.25
D_{30} (mm)	ASTMD-422	0.15
D_{10} (mm)	ASTMD-422	0.095
C_u	ASTMD-422	2.77
C_c	ASTMD-422	0.95
γs (kN/m^3)	ASTMD854-02	2.62
e_{max}	ASTMD4253-00	0.85
e_{min}	ASTMD4254-00	0.30
Es (%)	ASTM D2419	84.20
$CaCo_3$ content (%)	ASTM D4373-96	40

It is worth pointing out that polypropylene fibers are synthetic fibers that are made from synthetic polymers obtained from substances supplied by the petrochemical industry. Their mechanical and physical characteristics are summarized in the following table:

Table 2. Polypropylene fiber properties (Afitex Algérie)

Polypropylene properties	Results
Diameter (µm)	10-200
Length (mm)	6-18
Density	0,9
R_tMPa	400-750
E 10^3 MPa	5-10
Elongation at break in %	15-25
Coefficient of expansion (µ/m)	90
R_{fire} Max T. °C	150

Figure 3. Polypropylene fibers used for the reinforcement

Shaking Table Characteristics

Laboratory vibration testing aims essentially to monitor the variations in the behavior of soil that is placed in a plexiglass container. The experiments conducted in this study involved applying a seismic model to two density states, the first type in a loose state and the second in a medium-dense state. This was done in order to collect as much information as possible (Asmar et al., 2025). This step involved preparing and carrying out a test using a vibration table which consists of:

1. Quanser XY Shake TableIII
2. Power amplifier
3. Data acquisition (DAQ)
4. PC running there al-time control

Figure 4. Experimental devices

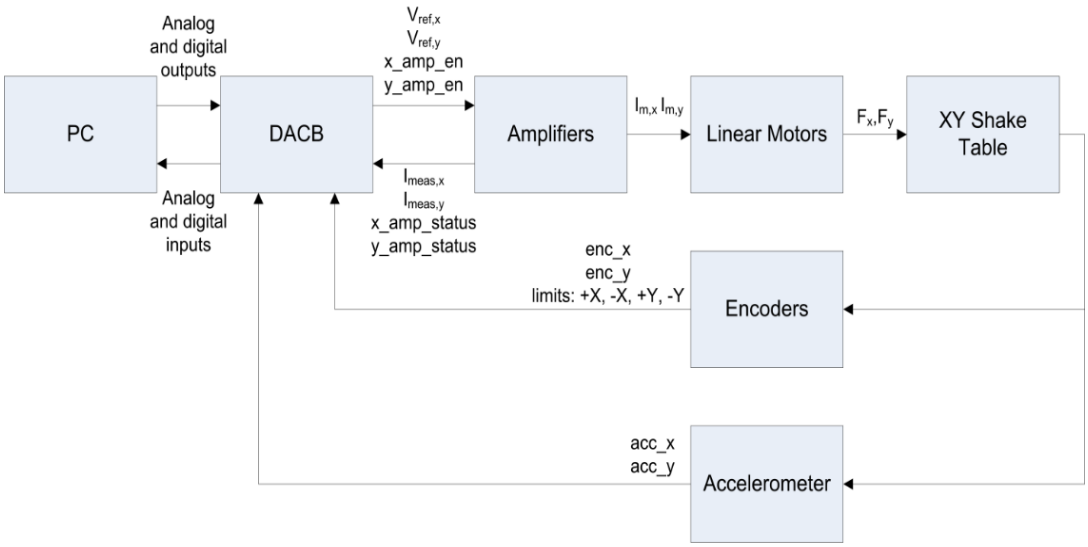

Figure 5. Interaction between main XY Shake Table III components

Thus, the results obtained from the tests will be used to calculate the accelerations and vertical displacements using a program developed in Matlab. In addition, frame-by-frame videos of the horizontal displacements of the table and the box were recorded. It should be noted that this box, which contains sand, is subjected to a horizontal seismic acceleration, in accordance with the 1999 Chi-Chi earthquake model (Mahmoudabadi et al., 2017). The real acceleration (10m/s²) is reduced by a factor of 10^{-3} (scale effect). The sample under study is placed in a transparent plexiglass cube of volume 20x20x20cm³. The height of the sample is 8 cm, while its weight is fixed according to the required relative density. The study aims to monitor the displacement of the intruder, placed on the top of the sample, according to the imposed relative density of soil.

To assess the effect of adding fibers of different lengths on the strength of sand in a static state, unconsolidated undrained triaxial tests were conducted on loose sand with a relative density Dr = 0%, and a medium-dense sand with Dr = 40%, as determined from Equation (1). The sand was confined at 100, 200 and 300 kPa and reinforced with 0.3% and 0.9% by mass of fibers for lengths equal to 6 mm and 12 mm.

$$D_r(\%) = \frac{e_{max} - e}{e_{max} - e_{min}} * 100 . \quad (1)$$

The tests were conducted on natural sand and fiber-reinforced sand using a triaxial shear apparatus. The objective of the triaxial shear test was to determine the mechanical characteristics of natural and reinforced sand. The tests were carried out on specimens 38 mm in diameter and 76 mm in height, with a slenderness ratio of 2. The shear rate used was 0.5 mm/min.

Characterization of Natural Sand and Reinforced Sand in Static Mode via Triaxial Path Tests, under Unconsolidated and Undrained Conditions

Effect of Fiber Percentage and Length on the Stress Deviatoric in Loose and Medium-dense Sand

Figure 6 shows the evolution of the deviatoric stress as a function of three confining pressures; namely, 100, 200, and 300 kPa, applied to two types of sand; i.e., loose sand and medium-dense sand, reinforced with 0.3% and 0.9% fibers, and with two different lengths; i.e., 6 mm and 12 mm. The results of the tests are reported in Tables 3 and 4 and the related data is presented in Figure 6.

Table 3. Results of the maximum deviatoric stress of loose sand (Dr=0%)

σ_3 (kPa)		**100**	**200**	**300**
F= 0%		395	634	950
6 mm	F = 0,3%	561	914	1100
	F = 0,9%	630	1112	1130
12 mm	F = 0,3%	590	950	846
	F = 0,9%	686	987	817

Table 4. Results of the maximum deviatoric stress of medium dense sand (Dr=40%)

σ_3 (kPa)		100	200	300
	F= 0%	540	946	1350
6 mm	F = 0,3%	600	1139	980
	F = 0,9%	738	1332	1020
12 mm	F = 0,3%	706	1407	1220
	F = 0,9%	790	810	715

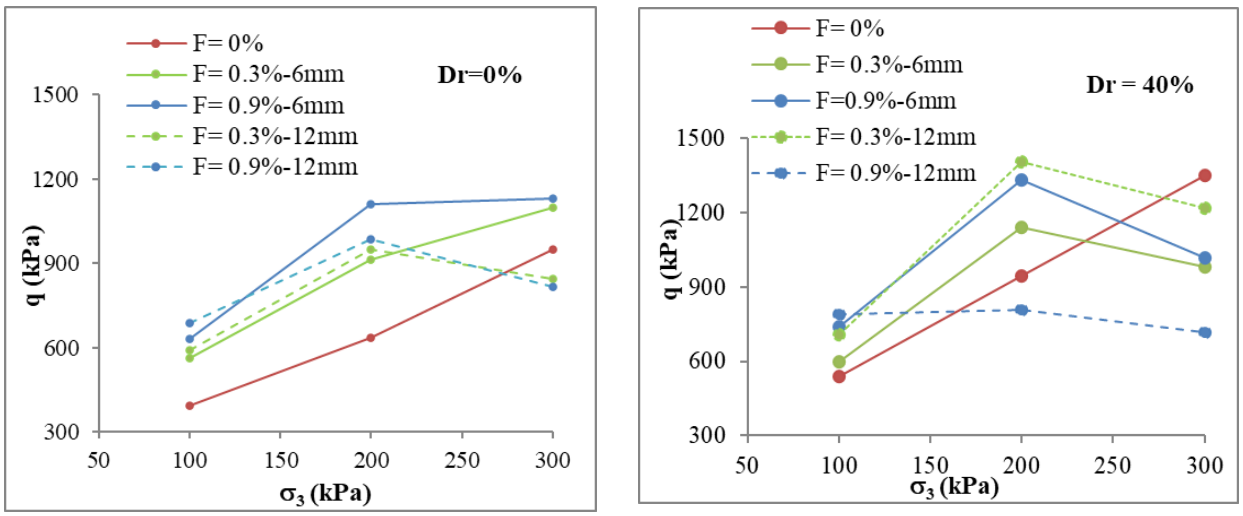

(a) (b)

Figure 6. Effect of fiber reinforcement on deviatoric stress of loose sand (a) and medium dense sand (b)

It is noticed that:

- For natural sand, in a loose or medium-dense state, both the deviatoric stress and density increase with confinement, because when the confining pressure is high, the voids in the soil closed quickly.
- For loose sand reinforced with 6-mm fibers, it was observed that the deviatoric stress increases with increasing fiber percentages. However, for 12 mm fibers, the deviatoric stress increases up to a confining pressure of 200 kPa, then starts decreasing. The results above are in accordance with the observations of other studies (Zhao et al., 2020; Li et al., 2022).
- For medium-dense sand reinforced with 6 mm fibers, the deviatoric stress increases with increasing fiber percentages, at confining pressure of 200 kPa, then begins to decrease.
- For medium-dense sand reinforced with 0.3% fibers with 12 mm length, the deviatoric stress increases up to a confining pressure of 200 kPa, then starts decreasing. In addition, the strength of medium-density sand reinforced with 0.9% fibers was found to be smaller than that of unreinforced natural sand. This can be explained by the fact that initially the soil structure is quite compact with fewer voids, and with the addition of fibers greater than 0.3%, the fibers form a ball, creating an area of low contact (ball effect).
- For medium-dense sand, confined at a pressure of 300 kPa, natural sand was found to be more resistant than reinforced sand.

Effect of Fiber Percentage and Length on Strength Gain for Loose and Medium-dense Sand

The evolution of strength gain due to fiber reinforcement is depicted in Figure 7. The percentage gain in strength is expressed as follows:

$$Gain(\%) = \left[\frac{qmaxR - qmaxN}{qmaxN}\right] * 100 \quad (2)$$

where:

- q_{maxR} is the peak deviatoric stress of reinforced sand, and
- q_{maxN} is the peak deviatoric stress of non-reinforced sand.

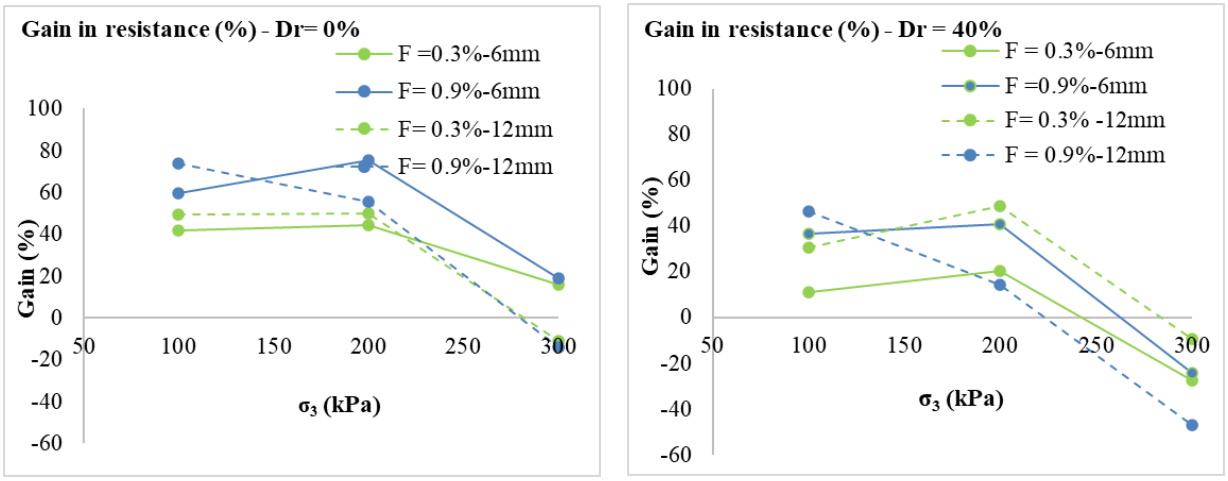

(a) (b)

Figure 7. Evolution of strength gain with multiple factors for loose density (a) and medium density (b)

Figure 7 shows the influences of the percentages and lengths of added fibers on the strength gain, for loose and medium-dense sand. It is then noted that:

- The strength gain increases as the percentage of added fibers and their length increase, for a confining pressure of100 kPa. However, this gain begins to decrease at a percentage of 0.3% of fibers with a length of 12 mm, and for a confining pressure of 300 kPa for both densities.
- For fibers with 6 mm length, the strength gain increases with the confining pressure up to 200 kPa. Then, it begins to decrease up to a confining pressure of 300 kPa, regardless of the density and percentage of added fibers. Figure 7 shows that the gain increased from 59.49% at 100 kPa confinement to 75.39% at 200 kPa, then decreased to 18.95% at 300 kPa for 0.9% fibers and 6 mm length. This means that adding fibers, regardless of their length, improves the strength gain at a certain level of confinement.
- For fibers at 0.9%, with a length of 12 mm, the strength gain reaches its maximum at a confining pressure of 100 kPa, for both densities; i.e., D_r = 0% and D_r = 40% and begins to decrease at a confining pressure of 300 kPa. This is because the length of the fibers affects the structure of the sand when they are longer, forming balls and being subjected to higher confinement (above 100 kPa), which weakens the contact between grains and between grains and fibers.
- The highest strength gain reached 75% for loose sand reinforced with 0.9% fibers of 6 mm length, and subjected to a confining pressure of 200 kPa. However, for medium-dense sand, the maximum strength gain reached 49% when this sand was reinforced with 0.3% fibers of 12 mm length, for a confining pressure of 200 kPa.
- The findings allow concluding that reinforcement with polypropylene fiber increases the ultimate strength of sand and enhances the strength gain. The results obtained showed that the ultimate strength can increase or decrease, depending on the percentage of fibers added and, on their length as well. The same results were observed by Hou et al. (2020) and Li et al. (2022).

Effect of Fiber Addition on the Ductility of Sands

In the context of geotechnical engineering, ductility refers to the ability of a material to deform plastically (without breaking) under stress. These results confirm that fiber addition affects positively the ductility of sand, which is in accordance with several studies (Michalowski & Cermak, 2003; Marandi, 2008; Nhema et al., 2021; Ghembaza et al., 2023). It has indeed been shown that fiber-reinforced sand is generally more ductile than natural sand. The results are summarized in Tables 5 and 6.

Table 5. Results of axial deformation for loose and medium-dense sand (length l=6mm)

6 mm	σ_3 = 100kPa			σ_3 = 200kPa		σ_3 = 300kPa	
Dr (%)	F (%)	q_{max} (kPa)	ε_1 (%)	q_{max} (kPa)	ε_1 (%)	q_{max} (kPa)	ε_1 (%)
0%	N	395	09.28	634	10.71	950	22.14
	0.3	561	11.42	914	12.5	1100	11.78
	0.9	630	13.57	1112	18.21	1130	16.78
40%	N	540	07.14	946	10.42	1350	14.28
	0.3	600	09.28	1139	12.5	980	21.78
	0.9	738	16.42	1332	23.92	1020	15.71

Table 6. Results of axial deformation for loose and medium-dense sand (length l=12mm)

6 mm	σ_3 = 100kPa			σ_3 = 200kPa		σ_3 = 300kPa	
Dr (%)	F (%)	q_{max} (kPa)	ε_1 (%)	q_{max} (kPa)	ε_1 (%)	q_{max} (kPa)	ε_1 (%)
0%	N	395	09.28	634	10.71	950	22.14
	0.3	590	17.85	950	11.42	846	38.21
	0.9	686	21.78	987	18.57	817	20.71
40%	N	540	7.14	946	10.42	1350	14.28
	0.3	706	16.42	1407	31.07	1220	15.71
	0.9	790	24.64	810	18.57	715	13.92

The main findings are as given below:

- For loose and medium-dense sand, the axial strain of natural sand (unreinforced sand) increases as the confining pressure increases. For Dr = 0%, ε_1 is equal to 9,28%, 10,71% and 22,14% for 100, 200 and 300 kPa, respectively (Table 5). However, it decreases as the density increases; the axial strain reached a deformation of 7,14%, 10.42% and 14.28% for 100, 200 and 300 kPa, respectively.
- For reinforced sand with 0.9% of fibers and 6mm length, the maximum axial strain of loose and medium-dense sand reached the value of 18,21% and 23,92%, representing the maximum deviator stress of 1112 kPa and 1332kPa for confining pressure of 200 kPa. Beyond this pressure, axial deformation decreased, and the sand became brittle due to the high pressure, creating a slip plane within the sample. However, for medium-dense sand reinforced with 0.3% fibers, the sand reached its maximum axial strain at a confining pressure of 300 kPa.
- The maximum axial strain for loose sand reinforced with 12 mm fibers is obtained for a reinforcement percentage of 0.9% fibers for confining pressures equal to 100 kPa and 200 kPa, and for a fiber percentage of 0.3% for a confining pressure of 300 kPa.
- The maximum axial strain in medium-dense sand is obtained with a fiber percentage of 0.9% and a confining pressure of 100 kPa. With confining pressures of 200 kPa and 300 kPa, the maximum axial strain is obtained with 0.3% fibers.

The same observations were made by many authors who concluded that the inclusion of fibers increases the axial strain significantly, and consequently the ductility (Marandi, 2008; Nhema et al., 2021).

RESULTS AND DISCUSSION

The final selection of fiber characteristics for sand reinforcement in vibrational mode was validated on the basis of the characterization results of sand on triaxial tests:

- For loose sand incorporating 6-mm fibers and reinforced with 0.9% fibers,
- For medium-dense sand incorporating 12 mm fibers and reinforced with 0.3% fibers. This result is consistent with those of several researchers (Akbulut et al., 2007; Zhao, 2020).

Evaluation of Dynamic Parameters of Natural Sand and Fiber-Reinforced Sand in Vibrational Mode

This work aims to conduct a series of vibration tests on a saturated, loose and medium-dense sand sample, with relative densities (D_r0 and D_r40) %. The objective is to gain some insight into the behavior of soil at different degrees of saturation, ranging from 50% to 100%.

The shake table shown in Figure 4 is a high-powered planar stage system that can move a load of up to 100 kg at high accelerations and velocities. The stage itself is capable of moving in either the X or Y directions and has a total travel greater than 20 cm on each axis. The interaction between the different components of the system is illustrated in Figure 5, and the experimental procedure was carried out following the flowchart presented in Figure 8. The simulated test carried out on the sand before and after the test is presented in Figure 9.

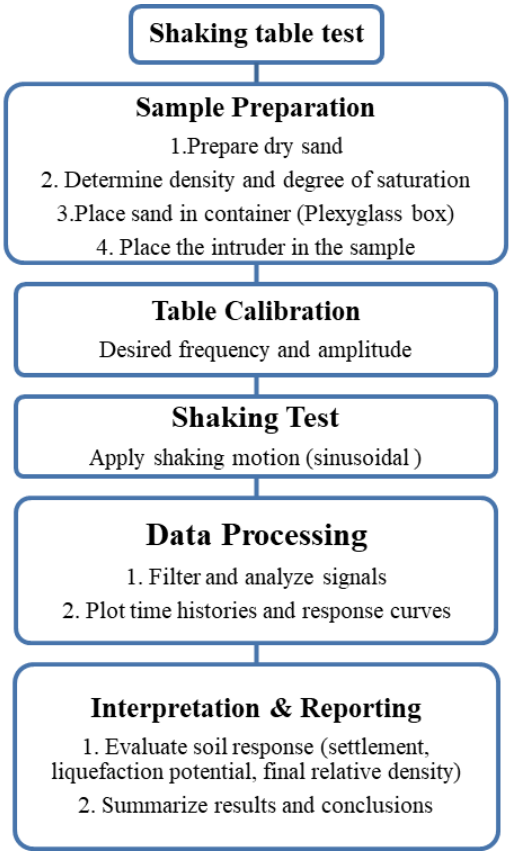

Figure 8. Flowchart of steps test

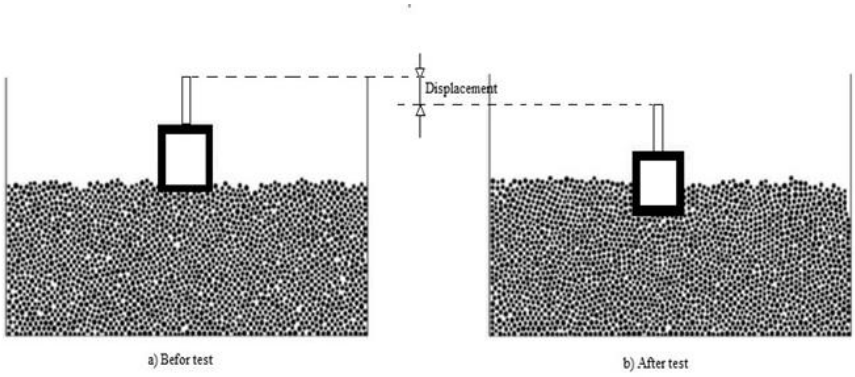

Figure 9. The position of the intruder before the test (a) and after the test (b)

The results for the vertical displacement of the intruder are presented in Figures from 10 to 14. For example, for a saturation degree of 80%, the loose sample exhibits a quite good behavior. In the case of reinforced sand, it was observed that the soil behavior improved by more than 60%.

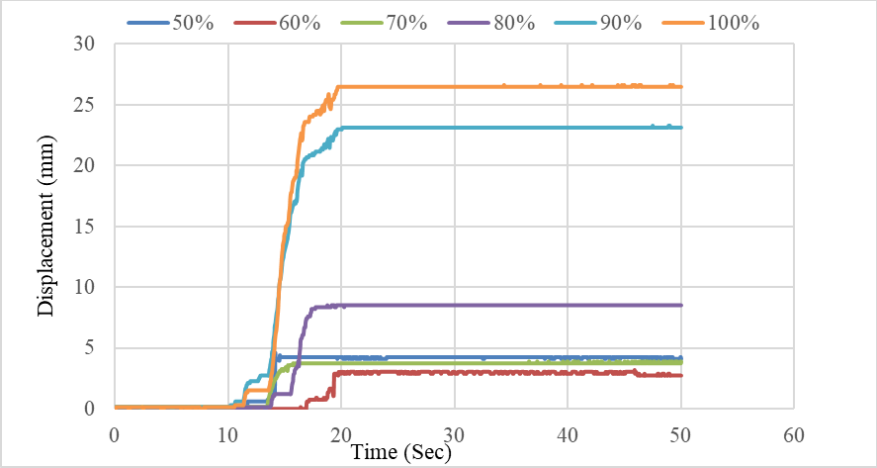

Figure 10. Results of vertical displacement Dr0 (without reinforcement)

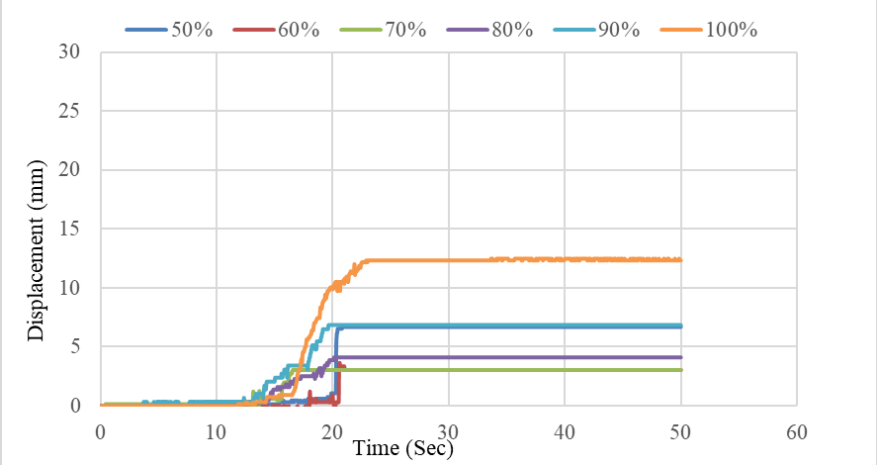

Figure 11. Results of vertical displacement Dr0 (with reinforcement)

The results corresponding to the variation of the final relative density (at the end of the test) as a function of the saturation degree are given in Tables 7 and 8.

Table 7. Test results with loose density Dr0

		Final Relative Density Drf	NOTE
Without reinforcement	50	27.5	Dry behavior
	60	35.8	Dry behavior
	70	42.5	Minimum variation
	80	62.5	Variation of Dr
Degree of saturation %	90	67.5	Excited behavior of the sample
	100	79.2	Excited behavior of the sample
with reinforcement	50	20.8	Dry behavior
	60	27.5	Dry behavior
Degree of saturation %	70	34.1	Minimum variation
	80	45.8	Minimum variation
	90	50.8	Minimum variation
	100	70.8	Variation of Dr

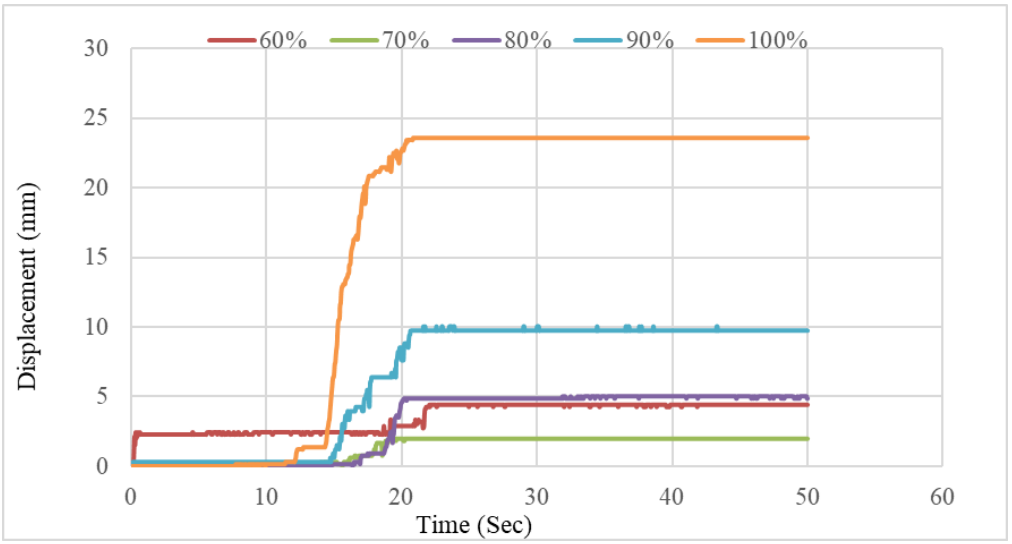

Figure 12. Results of vertical displacement Dr40 (without reinforcement)

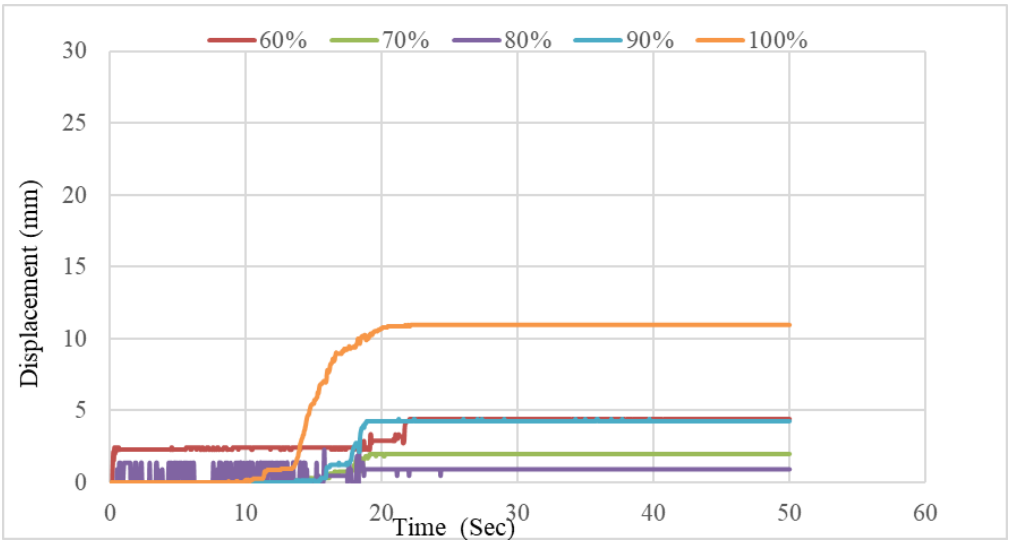

Figure 13. Results of vertical displacement Dr40 (with reinforcement)

Table 8. Test results with medium density Dr40

		Final Relative density D_{rf}	NOTE
without reinforcement Degree of saturation %	60	69.13	Dry behavior
	70	74.13	Minimum variation
	80	77.47	Variation of Dr
	90	82.47	Variation of Dr
	100	89.15	Excited behavior of the sample and the intruder
without reinforcement Degree of saturation %	60	50.77	Dry behavior
	70	54.11	Minimum variation
	80	57.45	Minimum variation
	90	64.12	Variation of Dr
	100	74.13	Variation of Dr

Results of the Correlation between the Final Relative Density and Saturation Degree

Figure 14 displays the correlation between the final relative density and saturation degree. The findings indicate that the fiber-reinforced sand exhibits better behavior, which gives it greater mechanical stability. In addition, it was found that the vertical displacement exceeds 22 mm for a saturation degree of 100% for unreinforced sand. However, for fiber-reinforced sand, the result is better, since this displacement does not exceed 12 mm, as clearly shown in Figures from 10 to 13. It can therefore be asserted that a clear improvement in behavior, of more than 50%, is observed, in the case of horizontal vibrations, for a 70% saturation degree and above.

The intruder penetrates the saturated sandy soil as the presence of water has liquefied its environment. It can therefore be said that the buoyancy force only applies in case of saturation. Its occurrence is often responsible for the vertical displacement of the intruder. The relative density at the end of the test varies proportionally with the increase in the degree of saturation of sand in loose and medium-dense states. Furthermore, when the saturation degree is less than 70%, the behavior of sand is identical to that of dry sand. In fact, the risk of liquefaction by rearrangement of grains occurs when the degree of saturation exceeds 70%. This risk exists when the intruder's displacement in the soil exceeds 10 mm. A similar study was conducted under constant vibration conditions by the EOST research team at the University of Strasbourg. The results obtained from vibration tests under constant frequency and amplitude on a soil sample reconstituted from synthetic beads (Clément et al., 2018 a, b) show that the soil behaves in the same way under vibration, with the first case exhibiting rigid behavior, the second heterogeneous fluid behavior and the third overall excitation based on constant acceleration imposed by the reduced model for a limited period of time.

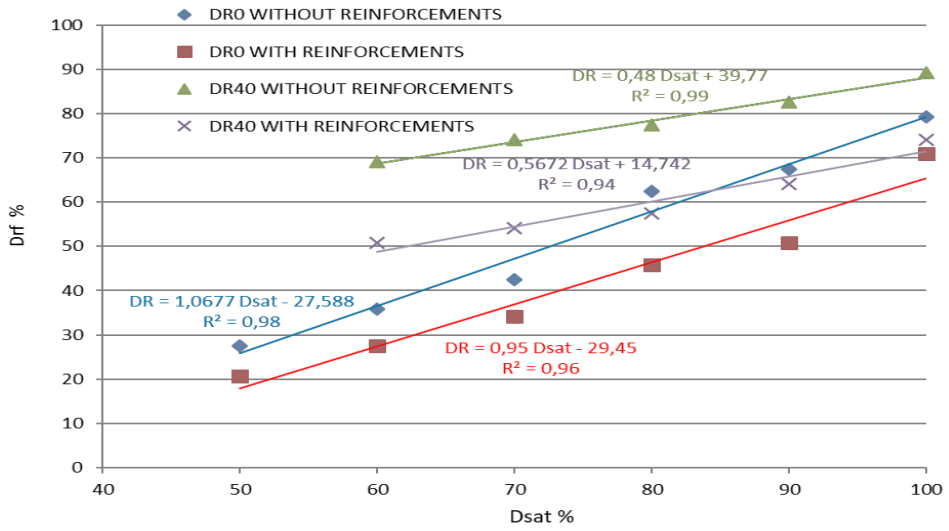

Figure14. Correlation results of final relative density and saturation

The variation in soil's relative density at the end of the test is proportional to the vibration amplitude. The relative density varies with acceleration and saturation (Equations from 3 to 6). Indeed, the risk of liquefaction depends on the rearrangement of sand grains. This risk is greater when the final relative density at the end of the test exceeds 40% of the initial relative density, as shown in Figure 14.

State 1: $Dsat \in [50,100]$ %

$$Drf = 1{,}07\ Dsat - 27{,}59 \quad \text{without reinforcement.} \quad (3)$$

$$\text{Drf} = 0{,}95\ \text{Dsat} - 29{,}45 \quad \text{with reinforcement.} \quad (4)$$

State 2: $\text{Dsat} \in [60,100]$ %

$$\text{Drf} = 0{,}48\ \text{Dsat} + 39.77 \quad \text{without reinforcement.} \quad (5)$$

$$\text{Drf} = 0{,}57\ \text{Dsat} + 14.74 \quad \text{with reinforcement.} \quad (6)$$

Finally, soil re-working is not proportional to the vertical displacement of the intruder when the soil exhibits unstable behavior.

CONCLUSIONS

The aim of this study is to improve the mechanical behaviour of saturated, undrained sand brought from the Port of Oran (Algeria) and subjected to horizontal vibrations according to the Chi-Chi earthquake model (Taiwan, 1999). The objective is to mitigate the risk of liquefaction. The findings of this study are presented as follows:

1. Liquefaction Susceptibility

The sandy soil under study was more susceptible to liquefaction when the degree of saturation was greater than 70% under seismic conditions.

2. Effectiveness of Fiber Reinforcement

Fiber inclusion significantly enhances the mechanical performance of sand. The most pronounced strength gain is observed in loose sand reinforced with 0.9% fibers of 6 mm length, while an optimal and acceptable improvement is achieved for medium-dense sand using 0.3% fibers of 12 mm length.

3. Deformation and Ductility Behavior

For loose sand, axial strain increases with both fiber content and confinement level. Overall, fiber reinforcement leads to higher axial strains, but markedly improves soil ductility, regardless of fiber length or confinement conditions.

4. Influence of the Initial Soil Conditions

Soil response is governed by initial soil conditions. Regardless of fiber reinforcement or initial relative density (Dr = 0% or 40%), the soil exhibits similar behavioral trends. Three distinct soil states were identified based on the variation between the final and the initial relative density (ΔDr) under seismic excitation:

- Static behavior state (ΔDr < 10%),
- Potential risk state (10% < ΔDr < 25%),
- Instability state characterized by a loss of strength (ΔDr > 25%).

5. Key Parameters Controlling Liquefaction Risk

The initial relative density and degree of saturation are critical parameters that control the behaviour of soil under seismic loading. The final relative density increases linearly with degree of saturation, and sands with saturation levels above 70% are particularly prone to liquefaction under seismic excitation. Fiber reinforcement effectively mitigates this risk, achieving an overall reduction of approximately 50%.

Acknowledgements

The authors sincerely thank the Editor-in-Chief and the anonymous reviewers for their valuable comments and careful evaluation, which significantly enhanced the clarity of the manuscript. They also extend their gratitude to Dr. Souad Amel Bourokba for her contribution to the manuscript's revision.

Notations and Symbols

C_c:Coefficient of curvature
CPT: Cone penetration tests
C_u: Coefficient of uniformity
D_i (mm): Grain diameter corresponding to *i*% finer
DP: Dynamic probing
*Dr:*Relative density
Dr0: Relative density at 0%, loose state
Dr40: Relative density at 40%, medium state
Dr_f: Final relative density %
Dsat: Degree of saturation %
e_{max}: Maximum void ratio (corresponding to loose state)
e_{min}: Minimum void ratio (corresponding to dense state)
E: Young's modulus
Gs or γ_s (g/cm^3): Specific weight of soil grains.
F = 0,3%: percentage with 0,3% of Polypropylene fibers
SPT: Standard Penetration Test
q: Deviatoric stress(kPa)
q_{max}: Peak deviatoric stress
Rt MPa: Tensile strength
R_{fire}: fire resistance
σ_3: Confining pressure (kPa)
ε_1 : Axial strain (%).

REFERENCES

Akbulut, S., Arasan, S., & Kalkan, E. (2007). Modification of clayey soils using scrap tire rubber and synthetic fibers. *Applied Clay Science, 38*(1-2), 23-32. https://doi.org/10.1016/j.clay.2007.02.001

Arab, A., & Shahrour, I. (2009, October 27-28). Effet de la saturation sur le comportement monotone et cyclique d'un sable [Effect of saturation on the monotonic and cyclic behavior of a sand]. In *Colloque international Sols non saturés et environnement (UNSATlemcen09)*, Tlemcen, Algeria.

Asmar, M.F.R., Harimurti, H., & Zaika, Y. (2025). Shaking table test on compacted soil to reduce liquefaction potential. *EUREKA: Physics and Engineering*, (1).

Beena, K.S., Jayakrishnan, V., Unni Kartha, G., & Shafnas, P. S. (2019). Studies on the effect of fines content on liquefaction resistance using shake table tests. In *Proceedings of the Indian Geotechnical Conference (IGC-2019)* (Vol. IV, pp. 723-735).

Benghalia, Y. (2018). *Étude expérimentale du comportement à la liquéfaction des sables des régions de Chlef et d'Alger* [Experimental study of the liquefaction behaviour of sands in the Chlef and Algiers regions]. *PhD Thesis*. University of BLIDA1.

Bouafia, A. (2010). *Introduction à la dynamique des sols: Volume II. Calcul dynamiques des ouvrages géotechniques* [Introduction to soil dynamics: Volume II. Dynamic calculations for geotechnical structures]. OPU, Algiers.

Bouaricha, L., & Djafar, H. A. (2015, October 19-20). Étude en laboratoire du comportement des sables-limon renforcé par des nappes en fibres de verre [Laboratory study of the behavior of sand-lime reinforced with glass fibre mats]. In *1er Séminaire international sur les routes et les matériaux routiers (RMR 2015)*, USTHB, Algiers, Algeria.

Bouaricha, L., Djafar, H.A., & Lancelot, L. (2019). Glass fiber effect on the undrained static response of Chlef sand (Northern Algeria). In *Recent advances in geo-environmental engineering, geomechanics and geotechnics, and geohazards* (Advances in Science, Technology & Innovation). https://doi.org/10.1007/978-3-030-01665-4_63

Boutouba, K. (2021). *Renforcement de sol par liant hydraulique: Analyse des caractéristiques mécaniques (expérimentation et modélisation)* [Reinforcement of soil by hydraulic binder: Analysis of mechanical characteristics (experimentation and modelling)] (Doctoral dissertation, Hassiba Benbouali University of Chlef, Algeria).

Brahim, A. (2017). *Évaluation en laboratoire de la performance d'un sable limoneux renforcé par fibres et géosynthétique* [Laboratory evaluation of the performance of a fibre-reinforced and geosynthetic silty sand] (Doctoral dissertation, Abdelhafid Boussouf University Centre of Mila, Algeria).

Chang, W. J., & Chou, S. H. (2019). Experimental study on shakedown compression of saturated granular soils due to pore pressure variation. *Journal of GeoEngineering, 14*(4), 9.

Cherif, T. A. (2017). *Étude en laboratoire de la susceptibilité à la liquéfaction des sables limoneux: Influence de la forme et taille des grains* [Laboratory study of liquefaction susceptibility of silty sands: Influence of grain shape and size] (Doctoral dissertation, Hassiba Benbouali University of Chlef, Algeria).

Clément, C., Toussaint, R., Stojanova, M., & Aharonov, E. (2018). Sinking during earthquakes: Critical acceleration criteria control drained soil liquefaction. *Physical Review E, 97*, 022905. https://doi.org/10.1103/PhysRevE.97.022905

Clément, C., Toussaint, R., & Aharonov, E. (2018). *Shake and sink: Liquefaction without pressurization* (arXiv:1802.04391). arXiv.

Della, N., Arab, A., Belkhatir, M., Missoum, H., & Bacconnet, C. (2010). Effet de la méthode de préparation sur le comportement non drainé d'un sol granulaire [Effect of the preparation method on the undrained behaviour of a granular soil]. *Revue Française de Géotechnique, 126-127*, 101-109. https://doi.org/10.1051/geotech/2009126101

El Ouni, M. R., Guettaya, I., & Ple, O. (2013). Évaluation du risque de liquéfaction de la fondation d'un barrage en terre à partir d'essais in situ [Assessment of the risk of liquefaction of the foundation of an earth dam based on in situ tests]. *Revue Française de Géotechnique, 143*, 31. https://doi.org/10.1051/geotech/2013143011

El Shamy, U., & Zeghal, M. (2007). A micro-mechanical investigation of the dynamic response and liquefaction of saturated granular soils. *Soil Dynamics and Earthquake Engineering, 27*(8), 712-729. https://doi.org/10.1016/j.soildyn.2006.12.010

Elzamel, A., Altahrany, A., & El-Meligy, M. (2023). Utilization of different additives in improving sandy

soil against liquefaction. *Jordan Journal of Civil Engineering, 17*(1), 107-116. https://doi.org/10.14525/JJCE.v17i1.10

Ghembaza, M. S., Bourokba, S., Hachichi, A., & Djeloul, R. (2023). Influence de la nature des fibres sur la résistance au cisaillement d'un sable limoneux [Influence of fiber type on the shear strength of silty sand]. *Algérie Équipement, 68*, 23-30.

Goren, L., Toussaint, R., Aharonov, E., Sparks, D. W., & Flekkøy, E. (2013). A general criterion for liquefaction in granular layers with heterogeneous pore pressure. In *Proceedings of the 5th Biot Conference on Poromechanics* (pp. 415-424).

Huang, Y., & Yu, M. (2017). *Hazard analysis of seismic soil liquefaction*. Springer. https://doi.org/10.1007/978-981-10-4379-6

Hou, T.S., Liu, J.L., Luo, Y.S., & Cui, Y.X. (2020). Triaxial compression test on consolidated undrained shear strength characteristics of fiber reinforced soil. *Soils and Rocks, 43*(1), 43-55. https://doi.org/10.28927/SR.431043

Ishihara, K. (1985). Stability of natural deposits during earthquakes. In *Proceedings of the 11th International Conference on Soil Mechanics and Foundation Engineering*.

Jeng, D.S., Ye, J.H., Zhang, J.S., & Liu, P.F. (2013). An integrated model for wave-induced seabed response under marine structures: Model verifications and applications. *Coastal Engineering, 72*, 11-19. https://doi.org/10.1016/j.coastaleng.2012.08.006

Kakaa, B., & Taki, M. (2008). Mechanical characterization of sand reinforced with different types of geotextiles. *Algérie Équipement, 44*.

Kousar, B., Ajay, V., & Abhilash, T. (2023, July). Assessment of initiation of soil liquefaction induced by earthquakes. *European Chemical Bulletin*, Special Issue 7, 2240-2259.

Leak, J., & Barreto, D. (2024). Particle size distribution induced fabric effects on the onset and post-liquefaction behaviors of soils. In *Proceedings of the XVIII European Conference on Soil Mechanics and Geotechnical Engineering*.

Li, L., Zhang, X., Xiao, H., Zhang, J., Chen, N., & Li, W. (2022). The triaxial test of polypropylene fiber reinforced fly ash soil. *Materials, 15*, 3807. https://doi.org/10.3390/ma15113807

Marandi, S. M., Bagheripour, M. H., Rahgozar, R., & Zare, H. (2008). Strength and ductility of randomly distributed palm fibers reinforced silty-sand soils. *American Journal of Applied Sciences, 5*, 209-220. https://doi.org/10.3844/ajassp.2008.209.220

Mahmoudabadi, V., Bahar, O., & Jafari, M. K. (2017). Identifying dynamic structural parameters of soil–structure system based on data recorded during strong earthquakes. *International Journal of Civil and Environmental Engineering, 11*(6).

Michalowski, R.L., & Cermak, J. (2003). Triaxial compression of sand reinforced with fibers. *Journal of Geotechnical and Geoenvironmental Engineering, 129*(2), 125-136. https://doi.org/10.1061/(ASCE)1090-0241(2003)129:2(125)

Nhema, C.C., Ke, H., Ma, P., Chen, Y., & Zhao, S. (2021). The influence of discrete fibers on mechanical responses of reinforced sand in direct shear tests. *Applied Sciences, 11*(19), 8845. https://doi.org/10.3390/app11198845

Nouri, S., Nechnech, A., & Lamiri, B. (2009). Comportement mécanique d'un sable renforcé par des nappes de polyéthylène [Mechanical behaviour of sand reinforced with polyethylene sheets]. In *Proceedings of the International Colloquium on Unsaturated Soils and the Environment (UNSAT Tlemcen 09)*, Algeria.

Nouri, S., Nechnech, A., & Lamiri, B. (2015). Étude expérimentale et modélisation numérique du comportement du sable renforcé par géosynthétiques [Experimental study and numerical modeling of geosynthetic-reinforced sand behavior]. *Algérie Équipement, 55*.

Ozbay, A., & Cabalar, A.F. (2016). Effects of triaxial confining pressure and strain rate on stick–slip behavior of a dry granular material. *Granular Matter, 18*, Article 60. https://doi.org/10.1007/s10035-016-0664-7

Santos, M. D., & Bicalho, K. V. (2022). Study of SPT–CPT and DP–CPT correlations for sandy soils. In *Cone Penetration Testing* (Gottardi & Tonni, Eds., pp. 677–682). https://doi.org/10.1201/9781003308829-99

Sawicki, A., & Mierczyński, J. (2009). On the behavior of liquefied soil. *Computers and Geotechnics, 36*(4), 531–536. https://doi.org/10.1016/j.compgeo.2008.11.002

Schlosser, F., Jacobsen, H.M., & Juran, I. (1984). Le renforcement des sols [Soil reinforcement]. *Revue Française de Géotechnique, 29*, 7-33. https://doi.org/10.1051/geotech/1984029007

Seed, R.B., Cetin, K.O., Moss, R. E. S., Kammerer, A. M., Wu, J., Pestana, J. M., & Reimer, M. F. (2001, March 26-31). Recent advances in soil liquefaction

engineering and seismic site response evaluation. In *Proceedings of the Fourth International Conference on Recent Advances in Geotechnical Earthquake Engineering and Soil Dynamics*, San Diego, CA, United States.

Shiva, P., & Kumar, K. (2018). Effect of randomly distributed fibre reinforcements on engineering properties of beach sand. *Jordan Journal of Civil Engineering, 12*(1), 99.

Sumer, B.M., Kirca, V.S.O., & Fredsøe, J. (2012). Experimental validation of a mathematical model for seabed liquefaction under waves. *International Journal of Offshore and Polar Engineering, 22*(2), 133-141.

Sun, F., Yao, Y., Li, X., Li, H., Chen, G., & Sun, Z. (2017). A numerical study on the non-isothermal flow characteristics of superheated steam in ground pipelines and vertical wellbores. *Journal of Petroleum Science and Engineering, 159*, 68-75. https://doi.org/10.1016/j.petrol.2017.09.014

Sun, F., Yao, Y., Li, G., & Li, X. (2018). Numerical simulation of supercritical-water flow in concentric-dual-tubing wells. *SPE Journal, 23*(6). https://doi.org/10.1016/j.petrol.2021.108790

Tsuchida, H. (1970). *Prediction and countermeasure against liquefaction in sand deposits*. Seminar of the Port and Harbour Research Institute, 1-33.

Yoshida, N. (2024). Definition of liquefaction. In *Proceedings of the 18th International Conference on Earthquake Geotechnical Engineering*. *Japanese Geotechnical Society Special Publication, 10*(12), 305-310. https://doi.org/10.3208/jgssp.v10.OS-1-01

Zhao, Y., Ling, X., Gong, W., Li, P., Li, G., & Wang, L. (2020). Mechanical properties of fiber-reinforced soil under triaxial compression and parameter determination based on the Duncan–Chang model. *Applied Sciences, 10*(24), 9043. https://doi.org/10.3390/app10249043